Original article formatted for *Molecular Ecology*

Genotyping-by-sequencing and ecological niche modeling illuminate phylogeography, admixture, and Pleistocene range dynamics in quaking aspen (*Populus tremuloides*)

Justin C. Bagley[1,2,*], Neander M. Heming[2], Eliécer E. Gutiérrez[2,3], Upendra K. Devisetty[4], Karen E. Mock[5], Andrew J. Eckert[1], and Steven H. Strauss[6]

[1]*Plant Evolutionary Genetics Laboratory, Department of Biology, Virginia Commonwealth University, 1000 W Cary St., TRANI 126, Richmond, VA 23284, USA*

[2]*Departamento de Zoologia, Instituto de Ciências Biológicas, Universidade de Brasília, 70910-900, Brasília, DF, Brazil*

[*]*Corresponding author.* E-mail: jcbagley@vcu.edu.

[3]*Programa de Pos-Graduação em Biodiversidade Animal, Centro de Ciências Naturais e Exatas, Universidade Federal de Santa Maria, Santa Maria, RS 97105-900, Brazil*

[4]*CyVerse, Bio5, University of Arizona, Keating Bioresearch Building, 0400D12, 1657 E. Helen St., Tucson, AZ 85721, USA*

[5]*Department of Wildland Resources and Ecology Center, Utah State University, 5230 Old Main Hill, Logan, UT 84322, USA*

[6]*Department of Forest Ecosystems and Society, Oregon State University, 321 Richardson Hall, Corvallis, OR 97331, USA*

Author E-mail Addresses: JCB: jcbagley@vcu.edu; NMH: neandermh@gmail.com; EEG: ee.gutierrez.bio@gmail.com; UD: upendra@cyverse.org; KM:

karen.mock@usu.edu; AJE: aeckert2@vcu.edu; SHS:

steve.strauss@oregonstate.edu.

Running Head: Quaking aspen phylogeography (28 characters w/spaces)

Contents: 8,177 words (Title, Abstract, & main text minus References and Table/Figure captions); 2 tables; 5 figures; and 11 Supporting Information files.

Keywords: admixture, North America, phylogeography, population structure, quaking aspen, single nucleotide polymorphisms (SNPs).

Abstract (249 words)

Populus tremuloides is the widest-ranging tree species in North America, and an ecologically important component of mesic forest ecosystems displaced by the Pleistocene glaciations. Using phylogeographic analyses of genome-wide SNPs (34,796 SNPs, 183 individuals) and ecological niche modeling, we inferred population structure, admixture, and Pleistocene range dynamics of *P. tremuloides*, and tested several historical biogeographical hypotheses. We found three genetic lineages located in coastal (cluster 1), Cascadian/Northern Rocky Mountains (cluster 2), and Southern Rocky Mountains to northern regions (cluster 3) of the *P. tremuloides* range, with phylogenomic relationships of the form ((cluster 1, cluster 2), cluster 3). The main vector of admixture was from cluster 3 into cluster 2, with the admixture zone trending northwest through the Rocky Mountains along a recognized phenotypic cline (Utah to Idaho). Clusters 1 and 2 provided mixed support for the 'stable-edge hypothesis' that unglaciated southwestern populations persisted *in situ* since the last glaciation. By contrast, cluster 3 exhibited 'trailing-edge' dynamics, e.g. clinal

genetic variation and niche suitability predictions signifying complete northward post-glacial expansion. Results were also consistent with the 'inland dispersal hypothesis' predicting post-glacial assembly of Pacific Northwestern forest ecosystems, but rejected the hypothesis that Pacific-coastal populations were colonized during outburst flooding from glacial Lake Missoula. Overall, congruent patterns between our phylogeographic and ecological niche modeling results and fossil pollen data demonstrate complex mixtures of stable-versus trailing-edge dynamics and refugial locations within *P. tremuloides*. These findings confirm and refine previous genetic studies, while strongly supporting a distinct Pacific-coastal genetic lineage of quaking aspen.

Introduction

Many North American forest tree species are broadly distributed across large areas of the continent (Little 1971; Prasad *et al.* 2007). Closely related populations and species also frequently occur across major geographical barriers, including western-Pacific mountain ranges (e.g. Cascades, Sierra Nevada), ranges of the greater continental divide (Rocky Mountains) and eastern divide (Appalachian Mountains), or xeric habitats of the Great Basin and major deserts. Explaining such distributions requires historical biogeographical processes of range fragmentation in a wide-ranging ancestral lineage spanning both sides of a barrier, and/or dispersal into areas on either side (e.g. Rosen 1978). Pleistocene glaciations represent another major factor influencing the distributions and genetic diversity of North American tree species (Hewitt 1996, 2001; Soltis *et al.* 2006; Jaramillo-Correa *et al.* 2009). Fossil pollen and plant macrofossil data show that the advance and retreat of massive continental ice sheets during the mid-late Pleistocene

cyclically reduced population sizes and forced extirpations of forest trees from northern glaciated areas, followed by predominantly northward population/range expansion during post-glacial recolonization (Jackson *et al.* 2000; Williams *et al.* 2004; but see Provan & Bennett 2008). Teasing apart these historical and evolutionary processes in a geographical context to explain the diversity, demography, and assembly of North American tree communities has been a key goal of phylogeography for more than 20 years (Sewell *et al.* 1996; Soltis *et al.* 1997; Mitton *et al.* 2000; Cheddadi *et al.* 2006; Fazekas & Yeh 2006; Godbout *et al.* 2008; O'Connell *et al.* 2008; Eckert *et al.* 2010; Gugger *et al.* 2010; Keller *et al.* 2010; Breen *et al.* 2012).

Quaking aspen, *Populus tremuloides* Michx., is the most widely distributed North American tree species, ranging from northern Canada southward into pockets of central Mexico (Fig. 1; Little 1971). While common above 500 m elevation, *P. tremuloides* occur in distinct microhabitats throughout their range, with montane western populations occurring in riparian corridor, treeline, and krümmholz stands (Shepperd *et al.* 2006) and eastern populations more likely encountered along rivers and riparian zones (Barnes & Wagner 2002). In addition to striking morphological variation (Barnes 1967, 1975), *P. tremuloides* possess among the highest genetic diversity reported for *Populus* species to date (e.g. Jelinski & Cheliak 1992; Cole 2005; Callahan *et al.* 2013; Wang *et al.* 2016), and genetic resources include linkage maps and a draft annotated genome (Pakull *et al.* 2009; Sjödin *et al.* 2009; Sundell *et al.* 2015). These characteristics make quaking aspen an ideal system for studying the genomic and ecological contexts of speciation and local adaptation in forest trees. Historically unglaciated portions of the species range correspond to major glacial-stage refugia in the Cascades/Northern Rocky Mountains and the mid-southern Rocky Mountain Front, based on phylogeographic data from many

plant and animal taxa (reviewed in Brunsfeld *et al.* 2001; Jaramillo-Correa *et al.* 2009). Therefore, *P. tremuloides* also presents outstanding opportunities for testing historical biogeographical hypotheses on the locations of forest tree refugia and the formation of mesic, temperate forest ecosystems of the Pacific Northwest and Rocky Mountains.

Several important gaps in our knowledge of *P. tremuloides* evolutionary history remain open to investigation, including whether additional data from high-throughput sequencing might confirm or refine previously described intraspecific genetic clusters (Callahan *et al.* 2013), and the nature of Pleistocene range dynamics [e.g. refugia since the Last Interglacial (LIG); but see Ding *et al.* (2017)] and their influence on intraspecific genetic variation. To address these knowledge gaps, we investigate the genetic structure and population history of *P. tremuloides* by integrating phylogeographical analyses of genotyping-by-sequencing (GBS) data (Elshire *et al.* 2011) with ecological niche modeling (ENM; Peterson *et al.* 2011) analyses predicting the species Pleistocene to recent geographical range-dynamics. Using a high ratio of genome-wide SNPs to individuals is an optimal sampling design (e.g. Felsenstein 2006) that has been shown to yield high-resolution inferences of population history, even with small–moderate sample sizes (e.g. Gutenkunst *et al.* 2009; Willing *et al.* 2012; Robinson *et al.* 2014; Boehm *et al.* 2015). Thus, we sought a balance between numerical and genomic sampling by offsetting losses of information from sampling on average ~ 5 (median: 3; range: 1–22) individuals per local subpopulation (=site) with thousands of unlinked single nucleotide polymorphism (SNP) loci from throughout the genome. Our specific goals were four-fold: 1) to infer broad-scale patterns of population structuring within *P. tremuloides* using genomic SNP data; 2) to test the presence and directionality of admixture between intraspecific gene pools; 3) to infer Pleistocene range dynamics of the species and its genetic lineages using

ENMs and assess whether genetic differentiation is explained by connectivity or isolation of predicted suitable habitats over the last glacial cycle; and 4) to test several a priori historical biogeographical hypotheses for North American forest trees described below.

Materials and Methods

Historical biogeographical hypotheses.—Our study design permitted testing two pairs of competing a priori historical biogeographical hypotheses, and one standalone hypothesis. First, we expected (H_1) the 'stable-edge hypothesis' of long-term persistence of *P. tremuloides* populations in the intermountain west to be strongly supported if predicted suitable areas were fully or partly stable from the LGM to present, had higher genetic or phylogeographic diversity (number of lineages), and exhibited significant isolation by geographical distance (Callahan *et al.* 2013; Hampe & Petit 2005). The opposite (H_2) 'trailing-edge hypothesis' would be supported if predicted suitable areas were completely latitudinally displaced during the LGM and populations exhibited clinal genetic patterns indicating large-scale post-glacial population expansions (e.g. Hewitt 1996, 2001; Hampe & Petit 2005; Excoffier *et al.* 2009). Based on previous studies, we expected stable-edge dynamics in 'southwestern cluster' populations and trailing-edge dynamics in 'northern cluster' populations of *P. tremuloides* (Callahan *et al.* 2013). *Populus tremuloides* also exhibits the 'mesic forest disjunct pattern' of Brunsfeld *et al.* (2001), with Pacific-coastal populations separated from interior Rocky Mountain populations by intervening arid habitats of the Columbia Plateau in east–central Washington. Thus, we used our genetic results to test two non-mutually exclusive regional biogeographical hypotheses proposed to explain this distributional pattern. We tested (H_3) the well-known 'ancient vicariance hypothesis' positing that Cascade/Costal range forests

became isolated from Northern Rocky Mountain forests during the Pliocene formation of the Cascades Range (Daubenmire 1975) against (H_4) the 'inland dispersal hypothesis' that mesic forests recolonized the Northern Rockies since the LGM without substantial genetic divergence from coastal populations (Brunsfeld *et al.* 2001; Brunsfeld & Sullivan 2005; Carstens *et al.* 2005). During post-glacial retreat of continental glaciers, large lakes formed and eventually overflowed, flooding to coastlines and sparking extirpations or dispersals of northern populations of plants and animals from the Pacific Northwest (Pielou 1991). Among the largest, glacial Lake Missoula in western Montana repeatedly flooded the eastern Washington scablands and inundated the Willamette Valley in Oregon and the Columbia Basin to the Pacific coast, with the most massive events occurring since ~20 ka, and most recently ~14.7 ka (Balbas *et al.* 2017, refs. therein). Thus we tested the 'Missoula floods hypothesis' that Pacific-coastal *P. tremuloides* populations were colonized by transfer of propagules during these latest pronounced Missoula floods, which would predict that at least some populations in coastal Oregon and Idaho–Montana exhibit genetic similarity.

Sampling and laboratory methods for genomic data.—We obtained samples of leaves or stem cuttings from 96 *P. tremuloides* trees from 33 local sites (1–5 trees per site) across the species native range in western North America (Fig. 1), including samples from 11 sites in Callahan *et al.* (2013). Additional information on the locations of the sampling sites and tissue sources of individual trees is provided in Data S1 of the Supporting Information. We extracted genomic DNA from tissues using an in-house, phenol–chloroform DNA extraction protocol available in our Mendeley Data accession. Presence and quantity of extracted DNA was quantified using a NanoDrop ND-1000 spectrophotometer (Thermo Fisher Scientific), and DNA quality was assessed by electrophoresis

on 1% agarose gels. DNA concentrations were normalized before a GBS library was prepared containing 96 multiplexed samples according to the genotyping-by-sequencing (GBS) protocol developed for maize (Elshire *et al.* 2011) using a 5-bp single-cutter restriction enzyme, *Ape*KI. Single-end sequencing generated 100-bp reads on a single lane of an Illumina HiSeq 3000 flowcell at the Center for Genome Research and Biocomputing at Oregon State University. Base calling was performed in Casava v1.8 (Illumina, San Diego, CA).

Dataset construction and bioinformatics.—To increase genome coverage and read depth for SNP discovery, we generated a final genome-wide dataset for analysis by complementing our novel Illumina GBS dataset above with a published *P. tremuloides* dataset from Schilling *et al.* (2014), obtained directly from the authors. Combining datasets was justified because Schilling *et al.* (2014) employed the same *Ape*KI GBS protocol used herein, with samples prepped in two multiplexed libraries each containing 96 individuals and sequenced on separate Illumina HiSeq 2000 lanes. Schilling *et al.*'s (2014) dataset comprised 107 samples from individuals (including 45 technical replicates) representing six additional subpopulations, including U.S. sites WWA, KFO, and MI and Canadian sites FLFL, HSPQ, and SPQ (details in Data S1).

We conducted reference-based assembly, SNP discovery, and genotyping using the TASSEL-GBSv2 pipeline (Glaubitz *et al.* 2014) in the TASSEL v5.0 software distribution (Bradbury *et al.* 2007). In TASSEL-GBSv2, unfiltered Illumina data were demultiplexed by barcode (removing sequences that mismatched barcodes), trimmed to 64 bp, and stored in bit format to reduce computational time. Identical reads were collated as haplotypes, or 'tags' (Lu *et al.* 2013). To allow singletons for improving demographic/gene flow inferences, we set the minimum k-mer count across taxa and read counts per tag to

1. For the reference genome, we used the updated annotated genome for *P. tremuloides* (v1.1, 'Potrs01b', 30.1 Mb of sequence) available from The Populus Genome Integrative Explorer website (http://www.popgenie.org/; Sjödin *et al.* 2009; Sundell *et al.* 2015). Reads were mapped to the reference genome based on sequence similarity using the Burrows-Wheeler alignment tool, bwa v0.7.17 (Li & Durbin 2009). SNPs were called from tag alignments starting at the same physical position along the reference genome and filtered using default 10% minimum locus coverage (proportion of individuals) and minimum 0.01 minor allele frequency (MAF) settings. We filtered these SNPs to generate a 'final' set of SNPs for downstream analyses by removing indels and four problematic individuals with low barcode assignment success, keeping only biallelic loci, requiring at least two individuals per allele (MAF = 0.0025), and removing SNPs with minimum locus coverage <50%, in vcftools v0.1.14 (Danecek *et al.* 2011). To evaluate potential effects of including technical replicates, we ran the SNP discovery pipeline a second time on the dataset while excluding technical replicates and compared the results to our original SNPs using Venn diagrams based on the output from vcf-compare (Danecek *et al.* 2011).

Population genetic diversity, structure, and admixture.—We used two methods to infer overall patterns of population genetic structure and individual ancestry from our final GBS SNPs. First, we used the model-based approach implemented in ADMIXTURE v1.3.0 to infer individual ancestries in a maximum-likelihood (ML) framework that outperforms STRUCTURE (Pritchard *et al.* 2000) in computational efficiency for large, genome-wide SNP datasets such as ours (Alexander *et al.* 2009). We estimated ancestry coefficients (Q) for each individual in 10 replicate ADMIXTURE runs for each of K = 1–10 current/ancestral gene pools or 'clusters'. We also performed two replicate runs of 50-fold cross-validation for K = 1–10 to determine potential error in ancestry

estimation of each K. We then plotted the errors and identified the K-value having the lowest cross-validation error as the best K. Second, we estimated genetic clusters and membership probabilities using the model-free discriminant analysis of principal components (DAPC; Jombart *et al.* 2010) method available in the adegenet R package (Jombart & Ahmed 2011). Unlike ADMIXTURE, DAPC does not make assumptions of panmixia within genetic clusters, or of linkage equilibrium among loci. We objectively identified the appropriate number of PCs using the 'xvalDapc' cross-validation procedure, which evaluates prediction success of using DAPC on a training set of 90% of observations from each local subpopulation to group the remaining 10% of observations (Jombart *et al.* 2010). Results were compared for the number of PCs minimizing mean squared error, and the maximum number of PCs with >90% prediction success.

We evaluated general patterns of genetic diversity by calculating observed (H_{O}) versus expected (H_{E}) heterozygosity, gene diversity (H_{S}), F_{IS}, and counts of heterozygote and singleton alleles on per-individual and per-locus bases, and compared these among local subpopulations and ADMIXTURE clusters. Calculations were conducted using vcftools (Danecek *et al.* 2011), adegenet (Jombart & Ahmed 2011), and hierfstat (Goudet 2005). Given that *P. tremuloides* likely experienced a drastic northward range expansion following the LGM (e.g. Jackson *et al.* 2000; Callahan *et al.* 2013), we tested for prevailing latitudinal or longitudinal clines in H_{O} and H_{S} (standardized for sampling effort by dividing population values through by sample size; hereafter, '$H_{\mathrm{O}}{}^{*}$' and '$H_{\mathrm{S}}{}^{*}$') using generalized linear models estimated in R for the species, and within each genetic cluster herein (see Results). We expected negative linear relationships in populations that experienced extensive post-glacial expansion consistent with the trailing-edge hypothesis (Hewitt 1996; Hampe & Petit 2005; Excoffier *et al.* 2009). We calculated

pairwise Nei's (1972) D and F_{ST} (unbiased estimator of Weir & Cockerham 1984) genetic distances between clusters and subpopulations in StAMPP (Pembleton *et al.* 2013). We assessed the differentiation of clusters further using a hierarchical analysis of genetic variance in hierfstat ('varcomp.glob' and 'boot.vc' functions), with trees ('ind') nested within local subpopulations ('pop'), nested within genetic clusters ('clust'), and significance of F-statistics estimated using 95% confidence intervals (CIs) from 100 bootstrap pseudoreplicates.

To evaluate spatial patterns of genetic variation and test the prediction of the stable-edge hypothesis that *P. tremuloides* populations from southwestern North America exhibit isolation by distance (IBD) due to long-term migration-drift equilibrium (Hampe & Petit 2005; Callahan *et al.* 2013), we tested for IBD using Mantel randomization tests and generalized linear modeling of linearized F_{ST} $[= F_{ST}/(1 - F_{ST})]$ versus log-geographic distance (after Rousset 1997). Tests used straight-line geographic distance between sampling locations estimated while accounting for the curvature of the earth's surface (Vincenty inverse solution) in Imap (Wallace 2012). Mantel significance ($\alpha = 0.05$) was assessed using 10,000 randomizations of the data in ade4 (Dray & Dufour 2007). IBD tests were conducted globally, and within each ADMIXTURE cluster.

Phylogenomic analyses with admixture.—Prior to phylogenomic analyses, we removed three individuals with more than ~50% missing data (CSS11, GCB5, and SFRG5-4-1, all from different populations; Data S1), yielding a dataset of 180 samples. We used TreeMix v1.13 (Pickrell & Pritchard 2012) to infer a maximum-likelihood tree topology of relationships among genetic clusters identified during our ADMIXTURE and DAPC analyses (see Results) while accounting for admixture among ancestral *Populus* populations. In the first set of analyses, where a *P. trichocarpa* outgroup sample was used to fix

the root, we accounted for linkage disequilibrium by using 500 bp blocks of SNPs, and a no-migration run was followed by a series of replicated runs sequentially adding migration events (−m flag). Migration edges were added until the proportion of variance in the SNP data explained by the model reached $\geq 99.8\%$ (Pickrell & Pritchard 2012). We evaluated the consistency and significance of migration edges by conducting five replicate runs at the final migration level while estimating standard errors of the migration weights. We estimated nodal support for the final topology using 500 bootstrapping pseudoreplicates with $k = 500$ bp blocks of contiguous SNPs, and we determined p-values indicating whether supported migration edges significantly improved the fit to the data using the default jackknifing procedure (Pickrell & Pritchard 2012). Support for migration edges or novel admixture patterns were also assessed using plots of the residual fit of the tree graph. We evaluated potential effects on our TreeMix results of the substantial proportion of missing data in the outgroup sample by re-running the TreeMix procedure above while excluding the outgroup sample, which produced unrooted tree topologies. We also conducted a performance analysis assessing the impacts of choice of k (block size) on our results, by reanalyzing the full dataset over the following range of k values: 10, 100, 250, 500, 750, 1000, 2000, and 5000 bp.

Ecological niche modeling.—We used *P. tremuloides* occurrence data from throughout the species native distribution from Worrall *et al.* (2013), as well as from our genetic sampling sites. As the dataset contained >100,000 occurrence records and such a large dataset would likely carry elevated geographical or environmental space biases (Reddy & Dávalos 2003; Boria *et al.* 2014), we decreased the number of records by spatially filtering occurrences located ≤10 km from other occurrences using the spThin R package (Aiello-Lammens *et al.* 2015). The filtered dataset comprised 14,146 occurrences and was

used in subsequent analyses. Our ENM analyses employed environmental data layers for 19 bioclimatic variables at a resolution of 2.5 decimal degrees, available in the WorldClim 1 dataset (Hijmans *et al.* 2005). The area used for calibration of the models was created as a 1.5° buffer around the minimum convex polygon encompassing all occurrence sites in the filtered dataset (*sensu* methods described in Anderson & Raza 2010; Barve *et al.* 2011).

To calibrate our models, we employed the maximum entropy method implemented in MaxEnt v3.3.3k76 (Phillips *et al.* 2006, 2017; Phillips & Dudík 2008). Given the importance of both evaluating model performance with spatially independent data and balancing model complexity and predictive power (Warren & Seifert 2011; Radosavljevic & Anderson 2014), we fine-tuned MaxEnt using ENMeval (Muscarella *et al.* 2014) accessed through the ENMwizard R package (Heming *et al.* 2018). We evaluated models using a geographic partition scheme, and we optimized two important MaxEnt parameters that impact model complexity and predictive power: the regularization multiplier (RM) and feature classes (FCs) (Muscarella *et al.* 2014). To optimize these MaxEnt parameters, we calibrated preliminary models employing a range of settings including the geographic 'block' partitioning scheme (Muscarella *et al.* 2014), but only varying the RM and FC values. We used 8 values of RM from 0.5 to 4.0, incremented by 0.5. For each RM, we conducted 15 preliminary analyses, one with each of the following feature classes or combination thereof: L, P, Q, H, LP, LQ, LH, PQ, PH, QH, LPQ, LPH, LQH, PQH, and LPQH, where 'L' is linear, 'P' is product, 'Q' is quadratic, and 'H' stands for hinge. In total, 120 preliminary models were built to select the best settings, including RM and FC combinations. Model selection was based on the small sample size-corrected Akaike information criterion (AICc) as the main optimality criterion. Model omission rates cal-

culated with the 10th percentile and minimum training presence thresholds, and the Area Under the receiver operating characteristic Curve (AUC), were also used as secondary criteria for model selection (Peterson *et al.* 2011; Warren & Seifert 2011). Selected MaxEnt parameters (Supporting Information file Data S2) were used to calibrate a final model using occurrences in the final filtered dataset, but without a geographic partition scheme. The final model was projected onto multiple climatic and paleoclimatic scenarios from late Pleistocene to present (Table 1) within a geographical area covering an extent of 12.5°–75.9° N and 47.0°–172.2° W.

We conducted a second set of ENM analyses to infer potential past to present geographical distributions of genetic clusters within *P. tremuloides* (see Results), and to test for different range shifts predicted under the stable- versus trailing-edge hypotheses. Calibration areas should not include regions that species/lineages cannot disperse to due to geographical or ecological barriers (Anderson & Raza 2010). Assuming intraspecific genetic clusters have similar dispersal capabilities, we defined calibration areas for each cluster by building minimum convex polygons using the coordinates of genetic sampling sites exclusive to each cluster. We also excluded areas pertaining to other clusters (for example, possible focal cluster absence due to competitive exclusion) and areas with species occurrences pertaining to unidentified lineages, i.e. areas not covered by our genetic sampling. Procedures were performed in R using ENMwizard and raster (Hijmans 2017) (see details in Supporting Information Appendix S1).

Results

Dataset construction, SNP discovery, and SNP filtering.—Sequencing our *Ape*KI GBS library and combining the raw reads with raw data from Schilling *et al.* (2014)

yielded a total of 634 million reads (see additional details in Appendix S1 of the Supporting Information). Reference-based assembly and SNP calling in the TASSEL-GBSv2 pipeline yielded a total of 52,410 SNPs representing 202 *Populus* individuals, and results were 99.4% similar to the initial SNPs when technical replicates were excluded (Venn diagram, Appendix S1). After filtering in vcftools and quality controls, the final variant set contained 34,796 SNP loci for 182 *P. tremuloides* individuals and one *P. trichocarpa* individual from a total of 36 sampling sites. The final dataset also contained considerable variation, with global F_{ST} and F_{IS} over all loci by subpopulation (Weir & Cockerham 1984) of 0.148 and 0.186, respectively. Most genetic variation was present in the ingroup, and removing the *P. trichocarpa* outgroup sample yielded nearly identical global F-statistics. Mean depth of coverage per final SNP locus (hence individual) was 13.95, but per-locus values ranged from ∼1 to 1091. Genetic diversity at these loci was moderate, for example with mean observed heterozygosity (H_O) of 0.13 and mean overall gene diversity (H_t) of 0.18 (see details in Table S1 of the Supporting Information).

Population genetic diversity, structure, and admixture.—Our ADMIXTURE and DAPC clustering analyses each identified three genetic clusters (Fig. 1). Cross-validation error estimates for the ADMIXTURE models decreased rapidly from $K = 1$ to reach a low point at $K = 3$, the 'best' K, and then increased steadily to higher levels (Fig. S1). In the final ADMIXTURE model (Fig. 1A), cluster 1 was located along the Pacific Northwestern coastal plain and Coast Range/Cascades in Washington and Oregon. Consistent with predictions of the inland dispersal hypothesis, H_4, cluster 2 had a disjunct distribution between the eastern Cascades/Sierra Nevada mountain ranges and the Northern Rocky Mountains, but exhibited limited genetic divergence (Figs. 1B–D). Cluster 3 was present across the remainder of the study area including areas east of the Northern Rock-

ies continental divide in the U.S. and Canada (Fig. 1C). Individuals in clusters 2 and 3, especially *P. tremuloides* from sites CSS, GCB, SFRG, POW, and MON had admixture proportions consistent with putative genomic backgrounds involving introgression (Q = 0.15–0.5 for at least one cluster). Also, the *P. trichocarpa* sample had admixture proportions equally divided between clusters 2 (Q = 0.48) and 3 (Q = 0.52). There were geographical gradients in Q-values indicating admixture between neighboring clusters and little or no admixture between disjunct clusters 1 and 3, with the exception being the CSS population from east–central Colorado, which had individuals partially assigned to all three clusters. The k-means clustering step of DAPC identified three clusters as the best solution based on the BIC inflection point (Fig. S2). During DAPC cross-validation, prediction success peaked at 20 retained PCs and remained above 90% up to 100 PCs, indicating that lower values optimally minimized error but retaining 100 PCs minimized error while maximizing information content (Fig. S3). DAPC results were identical across 20–100 PCs, and driven by the same SNPs in loading plots of each allele (e.g. Fig. S4); thus only results based on 100 PCs are presented. The final DAPC used two discriminant functions and yielded three clusters that were clearly differentiated along the first axis, matched the geographical pattern of the ADMIXTURE clusters (Fig. 1D), and were 95% similar to those from ADMIXTURE (see additional details in Appendix S1). Thus, we took the ADMIXTURE results as our best estimate of distinct genetic clusters and used them as a priori groups in subsequent genetic analyses.

Patterns of genetic diversity were consistent with deviations from Hardy–Weinberg equilibrium due to pronounced population structure in our dataset, with heterozygosity being substantial and similar among ADMIXTURE clusters (Fig. 3A) but lower than expected under random mating (Fig. 3C). Cluster 1 exhibited substantial heterozygosity,

relatively fewer singletons, and lower inbreeding F_{IS} consistent with limited admixture (Fig. 3B). By contrast, clusters 2 and 3 had relatively elevated inbreeding F_{IS}, possibly related to higher N_e or admixture levels. Cluster 3 also exhibited the lowest per-individual counts of singleton SNPs, or private genetic variation (Fig. 3). Re-analyses excluding putatively admixed cluster 2 and 3 edge populations ($Q_{max} < 0.75$) yielded nearly identical results (Fig. S5), indicating that hybridization likely has not biased our genetic diversity estimates. Additionally, while triploid *P. tremuloides* are common in intermountain west populations (Mock *et al.* 2012), we obtained higher cluster 2 and 3 F_{IS} values than we would expect under high triploid frequencies (Fig. 3B), even after excluding admixed populations (Fig. S5), suggesting triploidy likely has not substantially biased our heterozygosity estimates.

Nei's D estimates, F_{ST} estimates (Table S2), and heatmaps plotted against clustering trees of the distances (Figs. S6 and S7) suggested that cluster 2 was the most divergent from other clusters. Consistent with phylogenetic results below, F_{ST} was also lowest between clusters 1 and 2. Hierarchical genetic differentiation was moderate and significant between clusters relative to the whole species ($F_{clust/total} = 0.092$, 95% CIs: 0.090–0.094) and between populations within clusters ($F_{pop/clust} = 0.089$, 95% CIs: 0.088–0.091) (Table S3), and these two levels made relatively equal contributions to genetic variance partitioning among subpopulations ($F_{pop/total} = 0.173$, 95% CIs: 0.170–0.176).

In line with predictions of the stable-edge hypothesis, standardized ${H_O}^*$ and ${H_S}^*$ relationships with latitude and longitude were non-significant, indicating lack of a genetic signal of directional spatial expansions in clusters 1 and 2 in west–central portions of the species range (Fig. 5). Consistent with genetic predictions of trailing-edge hypothesis and genetic signatures of northward and eastward post-glacial expansions, our generalized

linear modeling results showed that standardized estimates of population genetic diversity significantly declined with longitude overall ($H_O{}^*$: $r^2 = 0.13$, $t = -2.23$, df = 32, $p = 0.03$; $H_S{}^*$: $r^2 = 0.15$, $t = -2.19$, df = 28, $p = 0.037$) and within cluster 3 ($H_O{}^*$: $r^2 = 0.53$, $t = -2.62$, df = 6, $p = 0.039$; $H_S{}^*$: $r^2 = 0.71$, $t = -3.14$, df = 4, $p = 0.035$) (Fig. 5). Genetic diversity within cluster 3 also exhibited a significant negative clinal relationship with increasing latitude ($H_S{}^*$: $r^2 = 0.66$, $t = -2.81$, df = 4, $p = 0.048$).

Contrasting previous results of Callahan *et al.* (2013), who reported significant IBD in their southwestern *P. tremuloides* cluster, we found no evidence for significant IBD overall, or within any of the ADMIXTURE clusters. Although linearized genetic distance declined with log-geographical distance in km between sites when analyzing the full dataset (Mantel's $r = -0.25$), the pattern was diffuse ($p = 0.99$; $r^2 = 0.063$). Relationships were even more diffuse but slightly positive during separate analyses of clusters 1–3 ($p > 0.05$, Mantel's r range = 0.07–0.23; Fig. S8 and Table 2).

Phylogenomic analyses with admixture.—The proportion of variance among our SNP loci explained by the tree graph estimated without migration in TreeMix was 99.7% and surpassed the target value of 99.8% when one migration edge was added ('m1' model; proportion of variance explained = 100%). Subsequent to this, five replicate runs using the final m1 model consistently yielded the same tree topology and a migration edge from ADMIXTURE cluster 3 into cluster 2 was significant in all runs ($p < 0.001$). The final m1 run that maximized the log likelihood of the model yielded a tree topology placing clusters 1 and 2 more closely related to one another than to cluster 3, and that was strongly supported by bootstrap proportions (Fig. 2A). The corresponding residual plot (Fig. 2B) agreed with patterns of admixture inferred from ADMIXTURE and DAPC results but suggested moderate admixture between cluster 1 and *P. trichocarpa* , despite

current crossability barriers between these species. The ingroup-only analysis excluding the outgroup sample (∼48% missing data) yielded a similar migration event from the ancestral cluster 3 population into cluster 2, with slightly different residuals (Fig. S9), suggesting that inclusion of this sample had no adverse effects. Likewise, TreeMix performance was similar over k values varying by two orders of magnitude for the analysis of the full dataset, indicating that results were insensitive to our choice of block size parameter to account for LD (Fig. S10).

Ecological Niche Modeling.—Our ENMeval analyses identified RM = 0.5 and a combination of product and hinge feature classes as the best-performing parameters for calibrating the final ENM. These parameters yielded a single 'best' candidate model with the lowest AICc score (135032.19) and an AICc weight of ∼1.0. This best-supported model had mean omission rates of 0.24 and 0.06 for the 10^{th} percentile and the lowest presence training thresholds, respectively, as well as a mean test AUC of 0.733. Values of these diagnostic metrics are provided for all candidate models in Supporting Information file Data S2.

Projecting the final model onto geographic space revealed large areas holding suitable conditions for *P. tremuloides* during the present, ∼6 ka in the Mid-Holocene (MH), and ∼125 ka during the LIG, whereas suitable climatic conditions for the species were restricted to a markedly smaller area ∼22 ka during the LGM (Figs. 4 and S11). During present-day, MH, and LIG periods, areas with suitable conditions for *P. tremuloides* showed a similar pattern, nearly all being located in northern North America and mainly covering modern-day Alaska, much of Canada, and small patches throughout the northwestern and western US (e.g. Fig. S11A, B, and D). By contrast, predicted suitable conditions for *P. tremuloides* during the LGM only occurred in areas of the modern-day

United States—mostly in the central and eastern U.S., but also in small scattered disjunct areas mainly throughout the southern Cascade Range, northern Sierra Nevadas, Great Basin, and south–central Rockies (Fig. S11C). These general patterns were consistently found in results based on different general circulation models (Table 1) and indicated an overall pattern of southward range contraction to one or more refugia in south–central areas of North America (Fig. 4).

The minimum convex polygon approach to defining areas for calibrating models of *P. tremuloides* clusters yielded areas from which $n = 11$, 45, and 1504 filtered occurrence points were extracted for clusters 1, 2, and 3, respectively (Appendix S1). Projecting final models for each cluster onto geographic space indicated that the overall pattern of range dynamics within *P. tremuloides* resulted from distinct late Pleistocene range shifts of the clusters relative to one another and to the species as a whole. Broadly consistent with the stable-edge hypothesis, cluster 1 predictions exhibited relative stability over the last glacial cycle, with contiguous or disjunct areas of high-predicted habitat suitability signaling refugial areas along the Pacific Northwestern coast, Olympic Peninsula, and Aleutian Islands (Fig. 4). By contrast, predicted suitable habitat areas for cluster 2 extended along coastal mountain ranges and the Northern Rockies for much of the late Pleistocene, but expanded to cover much of northern North America during the LGM and progressively contracted to its modern geographical range through an intermediate MH stage. Predicted interglacial (LIG and present) suitable areas for cluster 3 were scattered across the Rockies and parts of the Great Basin to the west, with a more or less contiguous area across southern Canadian boreal forests from Saskatchewan east to the Atlantic coast (Fig. 4). However, closely matching trailing-edge hypothesis predictions, LGM suitable areas for cluster 3 completely shifted to mid-latitudes in the continental

interior (similar to species-level results), with two minor potential refugial areas located to the west and east. Consistent with the inference of gene flow between clusters 2 and 3 in our TreeMix results, our paleodistribution modeling results inferred overlapping areas of suitable habitat for these two lineages during interglacial periods of the late Pleistocene, including LIG, MH and present-day areas in the Northern Rockies, Middle Rockies, and scattered areas of the intermountain west (Fig. 4). Suitable geographical areas for the genetic clusters were again consistently inferred across MaxEnt analyses, suggesting they were robust to differences among circulation models.

Discussion

We inferred the phylogeographic history of *Populus tremuloides* by combining broad-scale inferences of population structure and admixture based on genome-wide SNP data (Elshire *et al.* 2011) with spatially explicit predictions of the past to present geographical distributions of the species and its intraspecific lineages using ENM hindcasting (Waltari *et al.* 2007; Peterson *et al.* 2011). Under this framework, we found strong evidence for significant patterns of population divergence and admixture among three intraspecific genetic clusters. Our genetic and geospatial results also lent mixed support to the stable-edge hypothesis positing that 'rear edge' *P. tremuloides* populations persisted long-term in southwestern portions of the range since the LGM. By contrast, trailing-edge dynamics and canonical genetic predictions of post-glacial range expansion (e.g. clinal genetic variation; Hewitt 1996, 2001; Excoffier *et al.* 2009) were strongly supported overall and within cluster 3 (Callahan *et al.* 2013; Hampe and Petit 2005). These results agree with previous genetic findings of Callahan *et al.* (2013), but present a more nuanced picture of *P. tremuloides* evolution and diversification refining the geographical positions of genetic subdivisions, past or on-going admixture, and putative Pleistocene refugia.

Quaking aspen phylogeography, admixture, and Pleistocene range shifts.—Maximum-likelihood and model-free DAPC analyses strongly supported three intraspecific genetic clusters located in coastal (cluster 1), Cascades Range to Northern Rocky Mountains (cluster 2), and mid-southern Rocky Mountain to northern regions (cluster 3) of the *P. tremuloides* range (Figs. 1, 2, S1, S2 and S9). These clusters were significantly differentiated based on hierarchical F-statistics. The genetic and geographical distinctiveness of cluster 1 also supports a unique evolutionary history for the Pacific aspen populations, as suggested by taxonomists more than 100 years ago (Piper & Beattie 1915), and hence may warrant formal taxonomic recognition.

Following the divergence of *P. tremuloides* from a common ancestor with *P. trichocarpa*, our TreeMix species tree registered the deepest split between clusters 1 + 2 versus 3. This matches the principal genetic break reported in Callahan *et al.* (2013) based on microsatellite DNA markers and reveals our clusters 2 and 3 to be roughly analogous to their southwestern and northern clusters, respectively. However, Callahan *et al.*'s (2013) sampling in the zone between their main clusters was too sparse to clearly delineate the break beyond reference to the continental divide. We sequenced material from site POTR and two other sites near their break zone (BNF and their USF site, labeled SFRG herein) but also added samples from nearby stands in northeastern Washington, northwestern Montana, and Colorado. Probably due to our much broader sequencing of random nuclear loci from throughout the genome, piecemeal advances in geographical sampling coverage permitted us to redefine POTR as belonging to our southwestern cluster 2 rather than northern cluster 3, and to show that populations on a diagonal from northern Montana to central Colorado belong to cluster 3. Rather than strictly tracking the continental divide, the deepest genetic subdivision within *P. tremuloides* matches a

set of geological and elevational barriers in the Northern to Middle Rockies, but then deviates westward from the divide (which trends southward through central Colorado and western New Mexico), with the presumed barrier then correlating to cold xeric desert and shrubland habitats of the northern Great Basin and Snake River Plain.

A common Pleistocene biogeographical pattern in the Northern Hemisphere is isolation in allopatric refugia followed by post-glacial dispersal and secondary contact of independent evolutionary lineages (Avise 2000; Hewitt 2001; Swenson & Howard 2005). Cold desert regions of the break zone above agree well with the split between the "south-west-south" and "south-west-north" sub-clusters uncovered in Callahan *et al.* (2013), which they hypothesized to form a secondary contact zone in the eastern Great Basin. By contrast, we found individual admixture proportions within several populations (admixed individuals, left side of cluster 3 in Fig. 1A) indicating a zone of admixture or secondary contact between the cluster 2 and 3 lineages, but restricted to habitats along the Rocky Mountains, and our TreeMix analyses clarified the main direction of admixture as being from cluster 3 into 2 (Figs. 2, S9 and S10). We hypothesize that this putative area of hybridization spans from the Wasatch Range and Southern Rocky Mountains of Utah and Colorado (including sites SFRG and CSS) through the Northern Rockies (Bitterroot, Lewis, and Absaroka–Beartooth Ranges; including MON site) and into northern Idaho (POW site). Recent comparative analyses suggest that the Rocky Mountains represent a hotspot for phylogeographic breaks, hybrid zones, and contact zones across plant and animal taxa (Swenson & Howard 2005). This area, from southern Utah through northern Montana and Idaho, also corresponds to a known phenotypic cline in *P. tremuloides* leaf shape, size, and tooth number (Barnes 1975). Taken together, the intermediate SNP genotypes and clinal morphology of *P. tremuloides* in this region match theoretical

and empirical expectations for tension zones formed by secondary contact along physical barriers, with clines maintained not by steep environmental gradients but by a balance between dispersal and local adaptation (e.g. Barton & Hewitt 1985). A biogeographical scenario in which this zone was formed by post-glacial secondary contact is supported by generally disjunct areas of niche suitability of these lineages during the LGM, followed by predicted MH and present-day distributional overlap within the Rocky Mountains (Fig. 4), which may have facilitated gene flow since ∼6 ka. Several paleoecological records from the western US and Canada suggest that expansion and contact of cluster 2 and 3 lineages, if post-glacial, probably happened following ∼13 ka. First, fossil pollen records from Washington (Whitlock 1992), Alberta (Lichti-Federovich 1970), Wyoming (Whitlock 1993), and southeast to Utah (Howard 2016) do not indicate substantial (stable) percentages of *Populus* pollen in this area until ≤12–10 ka, when aspen joined pioneer forest and shrub communities that overtook preceding tundra and grassland/steppe habitats. Second, the final retreat of the Laurentide Ice Sheet opened an ice-free Canadian corridor by ∼13 ka, which was only recolonized northward by closed forests ∼5 ka (Lichti-Federovich 1970; Pielou 1991).

Stable- vs. trailing-edge dynamics and isolation by distance.—Testing for stable- versus trailing-edge dynamics (*cf.* Hampe & Petit 2005) is challenging, and distributional or genetic approaches alone are insufficient for distinguishing between multiple historical scenarios or processes that could produce similar patterns (e.g. Knowles *et al.* 2007; Gugger *et al.* 2010; reviewed by Gavin *et al.* 2014). As expected from previous genetic results (Callahan *et al.* 2013) and theoretical predictions that populations near refugial locations should harbor greater genetic diversity (Hewitt 1996, 2001; Excoffier *et al.* 2009), we recovered clear genetic imprints of post-glacial range expansion for *P. tremuloides* as a

whole and for cluster 3 (e.g. Figs. 3 and 5), supporting the trailing-edge hypothesis (H_2). These results are indirectly supported by spatially explicit predictions of Pleistocene suitable areas for *P. tremuloides* and its intraspecific clusters from ENM hindcasting (Fig. 4). While standardized genetic diversity showed significant relationships with longitude, the best genetic evidence for northward and eastward spatial-demographic expansions came from significantly negative clinal patterns of cluster 3 ${H_O}^*$ and ${H_S}^*$ with latitude and longitude, respectively (Fig. 5). These are precisely the patterns of expansion suggested by our ENM hindcasting results for *P. tremuloides* cluster 3 over LGM to present. These integrated genetic and ENM results agree with other studies of Pacific Northwestern plants that found reductions of genetic diversity during northward post-glacial expansions in perennials and conifers (reviewed by Soltis *et al.* 1997; Jaramillo-Correa *et al.* 2009). The inferred contraction of cluster 3 to a mid-continental glacial refugium likewise matches well with previous LGM–recent ENM hindcasting results (Ding *et al.* 2017) and paleobotanical records of *Populus* species shifting to cool mixed boreal and non-analog forests in the same area ~18 ka during the LGM and subsequently expanding northward to higher temperate latitudes with other arboreal species (e.g. *Alnus* and *Abies* pollen types; Jackson *et al.* 2000; Williams *et al.* 2004; Breen *et al.* 2012).

We found evidence of stable-edge dynamics in southwestern areas of the *P. tremuloides* range, including a greater diversity of phylogeographic lineages (Fig. 1), fully or partly stable niche suitability areas for clusters 1 and 2 over LGM–present (Fig. 4), and higher population genetic diversity in the west, with heterozygosity declining with longitude across the species range (Fig. 5). This supports Callahan *et al.*'s (2013) hypothesis that mountainous terrain promoted elevational range shifts consistent with stable-edge dynamics in southwestern *P. tremuloides* populations during the late Quaternary. How-

ever, support for stable-edge dynamics in clusters 1 and 2 was mixed, with the chief departure from expectations being a lack of significant isolation by distance (*sensu* Wright 1943) during Mantel tests (Mantel 1967) and linear modeling of genetic and geographic distances (Fig. S8 and Table 2). This outcome is difficult to interpret, given it could indicate that assumptions of IBD tests such as migration–drift genetic equilibrium or spatial and environmental homogeneity (in $\geq$1–2 dimensions) are not met for a particular gene pool. We interpret non-significant IBD test results for clusters 1 and 2 as suggesting that a stepping-stone or hierarchical model does not fit the data (e.g. Slatkin 1993; Bohonak 2002), and that a scenario of genetic drift within genetically cohesive clusters is too simplistic. If clusters 1 and 2 actually experienced stable-edge dynamics suggested by our genetic and ENM results, then this could be explained by local subpopulations experiencing varying levels of isolation and migration. For example, this could reflect the Cascadian–Northern Rockies disjunction seen in cluster 2 subpopulations, or clusters having low N_e or migration levels near range margins could have caused F_{ST} to become under-predicted by an IBD model (see McRae 2006). Still, cluster 1 exhibited greater variation in linearized F_{ST} than the other clusters, consistent with more ancient and genetically differentiated populations along stable edges (upper right, Fig. S8). We hypothesize that differences in the significance of IBD tests for the southwestern subpopulations between the two studies may be attributable to sampling artifacts caused by Callahan *et al.*'s (2013) inclusion of a highly disjunct Mexican subpopulation. Nevertheless, to obtain a better understanding of the effects of dispersal limitation in *P. tremuloides*, or potential for long-distance dispersal disrupting IBD patterns, we recommend additional studies extending our analyses of genome-wide SNPs to a greater density of southwestern subpopulations.

Biogeography of Pacific Northwest and Rocky Mountain mesic forests.—The question of how disjunct mesic forest species of the Pacific Northwest came to obtain their present distributions has long fascinated biogeographers (Daubenmire 1975; Brunsfeld *et al.* 2001; Brunsfeld & Sullivan 2005). While dominated by Douglas-fir and 'cedar–hemlock' forests interspersed with xerophytic pinelands (Brunsfeld *et al.* 2001), this ecosystem hosts three species of *Populus*—*P. angustifolia*, *P. tremuloides*, and *P. trichocarpa* (Little 1971; Eckenwalder 1996). *Populus tremuloides* cluster 2 exhibits a disjunct distribution between the Cascades/Sierra Nevada ranges and the Northern Rocky Mountains, which is a common forest pattern thought to be maintained by the action of arid shrubland/steppe habitats of the Columbia Plateau as a barrier to gene flow (Brunsfeld *et al.* 2001). Phylogeographic structuring and past Pleistocene niche suitability patterns inferred herein suggest that *P. tremuloides* cluster 2 entered this ecosystem and obtained a disjunct mesic forest distribution in the Pleistocene, after two major historical events impacted the region: 1) Pliocene uplift of the Cascades Range and 2) xerification of the Columbia Plateau ~2 million years ago (Ma) in the early Pleistocene (Daubenmire 1975; Brunsfeld *et al.* 2001). The chief reason for this is that, given Pleistocene glacial stages were much longer than relatively short ~10,000- to 20,000-year interglacials, the stability of *P. tremuloides* cluster 2 suitable areas in these mountain ranges over the last glacial cycle (Fig. 4) opens the possibility that the ancestral cluster 2 stock persisted in these areas during earlier glaciations over the last ~800,000 years (Pielou 1991; Lambeck *et al.* 2002). Nevertheless, we find limited genetic divergence between Cascade and Northern Rocky Mountain populations, as indicated by F_{ST}, Nei's D, and clustering tree topologies and heatmaps of the distances (Figs. 2, 3, S6 and S7), suggesting that major Plio–Pleistocene vicariant events above never sundered a continu-

ous ancestral population. Overall, these results reject the ancient vicariance hypothesis (H_3) but more closely resemble patterns of genetic variation expected under the inland dispersal hypothesis, our H_4 (e.g. Brunsfeld *et al.* 2001). Genetic predictions of the inland dispersal hypothesis have similarly been supported by previous phylogeographic results for other forest tree species (Carstens *et al.* 2005; O'Connell *et al.* 2008).

Our phylogeographic results also clearly demonstrate that catastrophic post-glacial floods that swept across the Pacific Northwestern landscape repeatedly during the Pleistocene likely have not played a major role in shaping population structuring within *P. tremuloides*. In contrast to initial predictions for the Missoula floods hypothesis, *P. tremuloides* from the Pacific coast and Idaho–Montana were classified by ADMIXTURE and DAPC into separate genetic clusters (Fig. 1). This is despite our ENM results for the LGM, under multiple paleoclimatic scenarios, showing that suitable habitat likely existed for P. tremuloides across the Columbia Basin and nearby regions from LGM to present, particularly for cluster 2 (Fig. 4). Moreover, if Missoula outburst flooding had transferred *P. tremuloides* from Montana to the Pacific coastal zone, we might expect similar patterns of admixture in these areas; however, this expectation was neither met by patterns of admixture coefficients (Fig. 1A) nor migration edges supported by multiple TreeMix analyses (Figs. 2, S9, and S10). We hypothesize that the formation and draining of post-glacial lakes including Missoula did not majorly impact *P. tremuloides* population structure due to the wind-dispersed nature and peculiar life-history strategy of this species (e.g. clonal stands throughout many western areas of the species range). Given evidence of an important effect of Missoula floods on cold-tolerant freshwater fishes and mammals (e.g. Miller *et al.* 2006; Young *et al.* 2017, refs. therein), we suggest that aquatic plants or rodent-dispersed tree species may be more likely to exhibit the genomic

signatures of such events, and thus might be more fruitful targets for future studies of outburst flooding effects on regional plant communities.

Comparative biogeography of North American *Populus*.—Our results yield a late Pleistocene biogeographical scenario for *P. tremuloides* starkly contrasting that proposed for some closely related *Populus* species, while resembling others. For example, balsam poplar, *P. balsamifera*, is thought to have persisted in a Beringian refugium whose genetic variation was subsequently swamped by post-glacial gene exchange with southern colonists (Breen *et al.* 2012), which possibly expanded northward from Central refugium source populations (Keller *et al.* 2010). By contrast, our ENM results indicate that *P. tremuloides* was probably never present in sheltered microhabitats or contiguous ice-free areas of the Beringian land bridge refuge during the last ice age (Fig. 4), as previously suggested for *P. balsamifera*. Results for *P. tremuloides* herein more closely resemble previous ENM hindcasting predictions for *P. trichocarpa*, which Levsen *et al.* (2012) found to suggest patterns of southern refugia and coastal stability, with northward post-glacial recolonization of Pacific Northwestern and Alaskan areas.

Acknowledgements

Research was crowdfunded through Experiment.com (https://experiment.com/projects/the-lost-aspens-of-the-willamette-valley-did-catastrophic-floods-carry-them-from-the-rockies), and we thank all 68 donors (Appendix S1) but recognize T. S. Leatherman for an especially generous donation. JCB received stipend support from U.S. NSF grant EF-1442486 to AJE, and NMH was supported by a postdoctoral fellowship from the Brazilian federal agency CAPES. K. House and N. Bruttell are thanked for articles in *The Oregonian* and *Corvallis Gazette-Times* popularizing the project. We thank E. R. Alverson (The Nature Conservancy), B. Ripple and K. Ault (Oregon State University), S. Gremel (National Park Service), K. Karoly (Lewis and Clark College),

and V. Hipkins and A. Chrisman (USDA Forest Service) for providing stand locations, DNA, or leaf material from aspen populations. We also recognize K. Vining (Oregon State University) and C. Zonick and A. Whitacre (Portland Metro) for conducting aspen collections, B. Greer for insights on aspen biogeography, and G. Meacham and J. F. Schmidt & Son Co. for support toward native aspen variety development using our genetic results.

References

Aiello-Lammens, M. E., Boria, R. A., Radosavljevic, A., Vilela, B., & Anderson, R. P. (2015). spThin: an R package for spatial thinning of species occurrence records for use in ecological niche models. Ecography, 38, 541–545.

Alexander, D. H., & Lange, K. (2011). Enhancements to the ADMIXTURE algorithm for individual ancestry estimation. BMC Bioinformatics, 12(1), 246.

Alexander, D. H., Novembre, J., & Lange, K. (2009). Fast model-based estimation of ancestry in unrelated individuals. Genome Research, 19, 1655–1664.

Anderson, R. P., & Raza, A. (2010). The effect of the extent of the study region on GIS models of species geographic distributions and estimates of niche evolution: preliminary tests with montane rodents (genus *Nephelomys*) in Venezuela. Journal of Biogeography, 37, 1378–1393.

Balbas, A. M., Barth, A. M., Clark, P. U., Clark, J., Caffee, M., O'Connor, J., Baker, V. R., Konrad, K., & Bjornstad, B. (2017). ^{10}Be dating of late Pleistocene megafloods and Cordilleran Ice Sheet retreat in the northwestern United States. Geology, 45(7), 583–586.

Barnes, B. V. (1967). Indications of possible mid-Cenozoic hybridization in the aspens of the Columbia Plateau. Rhodora, 69, 70–81.

Barnes, B.V. (1975). Phenotypic variation of trembling aspen in western North America. Forest Science, 21, 319–328.

Barnes, B. V., & Wagner, W. H. (2002). Michigan trees. The University of Michigan Press, Ann Arbor, MI.

Barton, N. H., & Hewitt, G. M. (1985). Analysis of hybrid zones. Annual Review of Ecology and Systematics, 16(1), 113–148.

Barve, N., Barve, V., Jiménez-Valverde, A., Lira-Noriega, A., Maher, S. P., Peterson, A. T., Soberón, J., & Villalobos, F. (2011). The crucial role of the accessible area in ecological niche modeling and species distribution modeling. Ecological Modelling, 222(11), 1810–1819.

Boehm, J. T., Waldman, J., Robinson, J. D., & Hickerson, M. J. (2015). Population genomics reveals seahorses (*Hippocampus erectus*) of the western mid-Atlantic coast to be residents rather than vagrants. PloS One, 10(1), e0116219.

Bohonak, A. J. (2002). IBD (isolation by distance): a program for analyses of isolation by

distance. Journal of Heredity, 93(2), 153–154.

Boria, R. A., Olson, L. E., Goodman, S. M., & Anderson, R. P. (2014). Spatial filtering to reduce sampling bias can improve the performance of ecological niche models. Ecological Modelling, 275, 73–77.

Bradbury, P. J., Zhang, Z., Kroon, D. E., Casstevens, T. M., Ramdoss, Y., *et al.* (2007). TASSEL: software for association mapping of complex traits in diverse samples. Bioinformatics, 23, 2633–2635.

Callahan, C. M., Rowe, C. A., Ryel, R. J., Shaw, J. D., Madritch, M. D., & Mock, K. E. (2013). Continental-scale assessment of genetic diversity and population structure in quaking aspen (*Populus tremuloides*). Journal of Biogeography, 40, 1780–1791.

Cheddadi, R., Vendramin, G. G., Litt, T., François, L., Kageyama, M., Lorentz, S., & Lunt, D. (2006). Imprints of glacial refugia in the modern genetic diversity of *Pinus sylvestris*. Global Ecology and Biogeography, 15(3), 271–282.

Cole, C. T. (2005). Allelic and population variation of microsatellite loci in aspen (*Populus tremuloides*). New Phytologist, 167(1), 155–164.

Danecek, P., Auton, A., Abecasis, G., Albers, C.A., Banks, E., DePristo, M.A., Handsaker, R.E., Lunter, G., Marth, G.T., Sherry, S.T., & McVean, G. (2011). The variant call format and VCFtools. Bioinformatics, 27, 2156–2158.

Ding, C., Schreiber, S. G., Roberts, D. R., Hamann, A., & Brouard, J. S. (2017). Post-glacial biogeography of trembling aspen inferred from habitat models and genetic variance in quantitative traits. Scientific Reports, 7(1), 4672.

Dray, S., & Dufour, A. B. (2007). The ade4 package: implementing the duality diagram for ecologists. Journal of Statistical Software, 22(4), 1–20.

Eckenwalder, J. E. (1996). Systematics and evolution of *Populus*. In: Biology of *Populus* and Its Implications for Management and Conservation. Edited by Stettler RF, Bradshaw HD, Heilman PE, Hinckley TM. NRC Research Press; pp. 7–32.

Eckert, A. J., van Heerwaarden, J., Wegrzyn, J. L., Nelson, C. D., Ross-Ibarra, J., González-Martínez, S. C., & Neale, D. B. (2010). Patterns of population structure and environmental associations to aridity across the range of loblolly pine (*Pinus taeda* L., Pinaceae). Genetics, 185(3), 969–982.

Elshire, R. J., Glaubitz, J. C., Sun, Q., Poland, J. A., Kawamoto, K., Buckler, E. S., & Mitchell, S. E. (2011). A robust, simple genotyping-by-sequencing (GBS) approach for high diversity species. PloS One, 6(5), e19379.

Excoffier, L., Foll, M., & Petit, R. J. (2009). Genetic consequences of range expansions. Annual Review of Ecology, Evolution, and Systematics, 40, 481–501.

Fazekas, A. J., & Yeh, F. C. (2006). Postglacial colonization and population genetic relationships in the *Pinus contorta* complex. Canadian Journal of Botany, 84, 223–234.

Felsenstein, J. (2006). Accuracy of coalescent likelihood estimates: do we need more sites, more sequences, or more loci? Molecular Biology and Evolution, 23, 691–700.

Gavin, D. G., Fitzpatrick, M. C., Gugger, P. F., Heath, K. D., Rodríguez-Sánchez, F., Do-

browski, S. Z., Hampe, A., Hu, F. S., Ashcroft, M. B., Bartlein, P. J., & Blois, J. L. (2014). Climate refugia: joint inference from fossil records, species distribution models and phylogeography. New Phytologist, 204(1), 37–54.

Gent, P. R., Danabasoglu, G., Donner, L. J., Holland, M. M., Hunke, E. C., Jayne, S. R., Lawrence, D. M., Neale, R. B., Rasch, P. J., Vertenstein, M., Worley, P.H., Yang Z-L., & Zhang, M. (2011). The community climate system model version 4. Journal of Climate, 24(19), 4973–4991.

Glaubitz, J. C., Casstevens, T. M., Lu, F., Harriman, J., Elshire, R. J., Sun, Q., & Buckler, E. S. (2014). TASSEL-GBS: a high capacity genotyping by sequencing analysis pipeline. PLoS One, 9(2), e90346

Godbout, J., Fazekas, A., Newton, C. H., Yeh, F. C., & Bousquet, J. (2008). Glacial vicariance in the Pacific northwest: evidence from a lodgepole pine mitochondrial DNA minisatellite for multiple genetically distinct and widely separated refugia. Molecular Ecology, 17, 2463–2475.

Goudet, J. (2005). Hierfstat, a package for R to compute and test hierarchical F-statistics. Molecular Ecology Resources, 5(1), 184–186.

Gugger, P. F., González-Rodríguez, A., Rodríguez-Correa, H., Sugita, S., & Cavender-Bares, J. (2010). Southward Pleistocene migration of Douglas-fir into Mexico: Phylogeography, ecological niche modeling, and conservation of "rear edge" populations. New Phytologist 189, 4, 1185–1199.

Hampe, A., & Petit, R.J. (2005). Conserving biodiversity under climate change: the rear edge matters. Ecology Letters, 8, 461–467.

Heming, N. M., Dambros, C., & Gutiérrez, E. E. (2018). ENMwizard: AIC model averaging and other advanced techniques in Ecological Niche Modeling made easy. R package version 0.1.7. Accessed at <https://github.com/HemingNM/ENMwizard>.

Hewitt, G. M. (1996). Some genetic consequences of ice ages, and their role in divergence and speciation. Biological Journal of the Linnean Society, 58(3), 247–276.

Hewitt, G. (2001). Speciation, hybrid zones and phylogeography - or seeing genes in space and time. Molecular Ecology, 10, 537–549.

Hijmans, R. J. (2017). Package 'raster': Geographic data analysis and modeling. R package version 2.6-7. Available at: <https://CRAN.R-project.org/package=raster>.

Hijmans, R. J., Cameron, S.E., Parra, J.L., Jones, P.G., & Jarvis, A. (2005). Very high resolution interpolated climate surfaces for global land areas. International Journal of Climatology, 25, 1965–1978.

Howard, K. A. (2016). A late Pleistocene to early Holocene climate, vegetation and fire history record for the Bonneville Basin, Utah, USA. Master's Thesis, The University of Utah, Logan, UT.

Jackson, S. T., Webb, R. S., Anderson, K. H., Overpeck, J. T., Webb III, T., Williams, J. W., & Hansen, B. C. (2000). Vegetation and environment in eastern North America during the last glacial maximum. Quaternary Science Reviews, 19(6), 489–508.

Jaramillo-Correa, J. P., Beaulieu, J., Khasa, D. P., & Bousquet, J. (2009). Inferring the past

from the present phylogeographic structure of North American forest trees: seeing the forest for the genes. Canadian Journal of Forest Research, 39(2), 286–307.

Jelinski, D. E., & Cheliak, W. M. (1992). Genetic diversity and spatial subdivision of *Populus tremuloides* (Salicaceae) in a heterogeneous landscape. American Journal of Botany, 79(7), 728–736.

Jombart, T., & Ahmed, I. (2011). Adegenet 1.3-1: new tools for the analysis of genome-wide SNP data. Bioinformatics, 27, 3070–3071.

Jombart, T., Devillard, S., & Balloux, F. (2010). Discriminant analysis of principal components: a new method for the analysis of genetically structured populations. BMC Genetics, 11(1), 94.

K-1 model developers (2004). K-1 Coupled GCM (MIROC) Description, K-1 Technical Report No.1. Center for Climate System Research (Univ. of Tokyo), National Institute for Environmental Studies, and Frontier Research Center for Global Change. Available at: <http://ccsr.aori.u-tokyo.ac.jp/~hasumi/miroc_description.pdf> (accessed on April 26, 2017).

Kageyama M, Braconnot P, Bopp L, Caubel A, Foujols MA, Guilyardi E, Khodri M, Lloyd J, Lombard F, Mariotti V, Marti O, Roy T, Woillez MN (2013a) Mid-Holocene and Last Glacial Maximum climate simulations with the IPSL model. Part I: comparing IPSL CM5A to IPSL CM4. Clim Dyn. doi: 10.1007/s00382-012-1488-8.

Kageyama M, Braconnot P, Bopp L, Caubel A, Foujols MA, Guilyardi E, Khodri M, Lloyd J, Lombard F, Mariotti V, Marti O, Roy T, & Woillez MN (2013b) Mid-Holocene and Last Glacial Maximum climate simulations with the IPSL model. Part II: model-data comparisons. Clim Dyn. doi: 10.1007/s00382-012-1499-5.

Keller, S., Olson, M., Silim, S., Schroeder, W. & Tiffin, P. (2010). Genomic diversity, population structure and migration following rapid range expansion in the balsam poplar, *Populus balsamifera*. Molecular Ecology, 19, 1212–1226.

Knowles, L. L., Carstens, B. C., & Keat, M. L. (2007). Coupling genetic and ecological-niche models to examine how past population distributions contribute to divergence. Current Biology, 17, 940–946.

Lambeck, K., Esat, T. M., & Potter, E. K. (2002). Links between climate and sea levels for the past three million years. Nature, 419(6903), 199–206.

Levsen, N. D., Tiffin, P., & Olson, M. S. (2012). Pleistocene speciation in the genus *Populus* (Salicaceae). Systematic Biology, 61(3), 401–412.

Li, H., & Durbin, R. (2009). Fast and accurate short read alignment with Burrows-Wheeler transform. Bioinformatics, 25(14), 1754–1760.

Lichti-Federovich, S. (1970). The pollen stratigraphy of a dated section of Late Pleistocene lake sediment from central Alberta. Canadian Journal of Earth Sciences, 7(3), 938–945.

Little, E. L. Jr. (Ed.) (1971). Vols. Miscellaneous Publication 1146. Digitized 1999 by US Geological Survey. US Department of Agriculture.

Lu, F., Lipka, A. E., Glaubitz, J., Elshire, R., Cherney, J. H., *et al.* (2013) Switchgrass genomic diversity, ploidy, and evolution: novel insights from a network-based SNP discovery

protocol. PLoS Genetics, 9(1), e1003215.

McRae, B. H. (2006). Isolation by resistance. Evolution, 60(8), 1551–1561.

Miller, M. P., Bellinger, M. R., Forsman, E. D., & Haig, S. M. (2006). Effects of historical climate change, habitat connectivity, and vicariance on genetic structure and diversity across the range of the red tree vole (*Phenacomys longicaudus*) in the Pacific Northwestern United States. Molecular Ecology, 15, 145–159.

Mock, K. E., Callahan, C. M., Islam-Faridi, M. N., Shaw, J. D., Rai, H. S., Sanderson, S. C., Rowe, C. A., Ryel, R. J., Madritch, M. D., Gardner, R. S., & Wolf, P. G. (2012). Widespread triploidy in western North American aspen (*Populus tremuloides*). PLoS One, 7(10), e48406.

Muscarella, R., Galante, P. J., Soley-Guardia, M., Boria, R. A., Kass, J. M., Uriarte, M., & Anderson, R. P. (2014). ENMeval: an R package for conducting spatially independent evaluations and estimating optimal model complexity for MAXENT ecological niche models. Methods in Ecology and Evolution, 5, 1198–1205.

O'Connell, L. M., Ritland, K., & Thompson, S. L. (2008). Patterns of post-glacial colonization by western red cedar (*Thuja plicata*, Cupressaceae) as revealed by microsatellite markers. Botany, 86, 194–203.

Otto-Bliesner, B.L., Marshall, S.J., Overpeck, J.T., Miller, G.H. & Hu, A, CAPE Last Interglacial Project members. (2006). Simulating Arctic climate warmth and icefield retreat in the last interglaciation. Science, 311(5768), 1751–1753.

Pakull, B., Groppe, K., Meyer, M., Markussen, T., & Fladung, M. (2009). Genetic linkage mapping in aspen (*Populus tremula* L. and *Populus tremuloides* Michx.). Tree Genetics & Genomes, 5(3), 505–515.

Peterson, A. T., Soberón, J., Pearson, R. G., Anderson, R. P., Martínez-Meyer, E., Nakamura, M., & Araújo, M. B. (2011). Ecological niches and geographic distributions. Princeton University Press.

Phillips, S. J., Anderson, R. P., Dudík, M., Schapire, R. E., & Blair, M. E. (2017). Opening the black box: an open-source release of Maxent. Ecography, 40(7), 887–893.

Phillips, S. J., Anderson, R. P., & Schapire, R. E. (2006). Maximum entropy modeling of species geographic distributions. Ecological Modelling, 190, 231–259.

Phillips, S. J., & Dudík, M. (2008). Modelling of species distributions with Maxent: new extensions and a comprehensive evaluation. Ecography, 31, 161–175.

Pickrell, J. K., & Pritchard, J. K. (2012). Inference of population splits and mixtures from genome-wide allele frequency data. PLoS Genetics, 8(11), e1002967.

Pielou, E. C. (1991). After the Ice Age: the Return of Life to Glaciated North America. University of Chicago Press, Chicago.

Piper, C. V., & Beattie, R. (1915). Flora of the northwest coast. New Era Printing Company, Lancaster, PA.

Prasad, A. M., Iverson, L. R., Matthews, S., & Peters, M. (2007). A climate change atlas for 134 forest tree species of the eastern United States [database]. Retrieved from US Department

of Agriculture, Forest Service website: http://www.nrs.fs.fed.us/atlas/tree.

Pritchard, J. K., Stephens, M., & Donnelly, P. (2000). Inference of population structure using multilocus genotype data. Genetics, 155, 945–959.

Provan, J., & Bennett, K. D. (2008). Phylogeographic insights into cryptic glacial refugia. Trends in Ecology & Evolution, 23(10), 564–571.

Radosavljevic, A., & Anderson, R. P. (2014). Making better Maxent models of species distributions: complexity, overfitting and evaluation. Journal of Biogeography, 41, 629–643.

Reddy, S., & Dávalos, L. M. (2003). Geographical sampling bias and its implications for conservation priorities in Africa. Journal of Biogeography, 30(11), 1719–1727.

Robinson, J., Bunnefeld, L., Hearn, J., Stone, G., & Hickerson, M. J. (2014). ABC inference of multi-population divergence with admixture from un-phased population genomic data. Molecular Ecology, 18, 4458–4471.

Rosen, D. E. (1978). Vicariant patterns and historical explanation in biogeography. Systematic Zoology, 27, 159–188.

Rousset, F. (1997). Genetic differentiation and estimation of gene flow from F-statistics under isolation by distance. Genetics, 145, 1219–1228.

Schilling, M. P., Wolf, P. G., Duffy, A. M., Rai, H. S., Rowe, C. A., Richardson, B. A., & Mock, K. E. (2014). Genotyping-by-sequencing for *Populus* population genomics: an assessment of genome sampling patterns and filtering approaches. PLoS One, 9(4), e95292.

Shepperd, W. D., Rogers, P. C., Burton, D., & Bartos, D. L. (2006). Ecology, Biodiversity, Management, and Restoration of Aspen in the Sierra Nevada. Gen. Tech. Rep. RMRS-GTR-178 (122 pp.). U.S. Department of Agriculture, Forest Service, Rocky Mountain Research Station, Fort Collins, CO.

Sjödin, A., Street, N. R., Sandberg, G., Gustafsson, P., & Jansson, S. (2009). The Populus Genome Integrative Explorer (PopGenIE): a new resource for exploring the *Populus* genome. New Phytologist, 182(4), 1013–1025.

Slatkin, M. (1993). Isolation by distance in equilibrium and non-equilibrium populations. Evolution, 47, 264–279.

Soltis, D., Gitzendanner, M., Strenge, D., & Soltis, P. (1997). Chloroplast DNA intraspecific phylogeography of plants from the Pacific Northwest of North America. Plant Systematics and Evolution, 206, 353–373.

Soltis, D. E., Morris, A. B., McLachlan, J. S., Manos, P. S., & Soltis, P. S. (2006). Comparative phylogeography of unglaciated eastern North America. Molecular Ecology, 15(14), 4261–4293.

Stevens, B., Giorgetta, M., Esch, M., Mauritsen, T., Crueger, T., Rast, S., Salzmann, M., Schmidt, H., Bader, J., Block, K., & Brokopf, R. (2013). Atmospheric component of the MPI-M Earth system model: ECHAM6. Journal of Advances in Modeling Earth Systems, 5(2), 146–172.

Sundell, D., Mannapperuma, C., Netotea, S., Delhomme, N., Lin, Y.-C., Sjödin, A., Van de Peer, Y., Jansson, S., Hvidsten, T. R., & Street, N. R. (2015). The plant genome integrative

explorer resource: PlantGenIE.org. New Phytologist, 208(4), 1149–1156.

Swenson, N. G., & Howard, D. J. (2005). Clustering of contact zones, hybrid zones, and phylogeographic breaks in North America. The American Naturalist, 166(5), 581–591.

Waltari, E., Hijmans, R. J., Peterson, A. T., Nyari, A. S., Perkins, S. L., & Guralnick, R. P. (2007). Locating Pleistocene refugia: comparing phylogeographic and ecological niche model predictions. PLoS One, 2(7), e563.

Wang, J., Street, N. R., Scofield, D. G., & Ingvarsson, P. K. (2016). Natural selection and recombination rate variation shape nucleotide polymorphism across the genomes of three related *Populus* species. Genetics, 202(3), 1185–1200.

Warren, D. L., & Seifert, S. N. (2011). Ecological niche modeling in Maxent: the importance of model complexity and the performance of model selection criteria. Ecological Applications, 21, 335–342.

Weir, B. S., & Cockerham, C. C. (1984). Estimating *F*-statistics for the analysis of population structure. Evolution, 38(6), 1358–1370.

Whitlock, C. (1992). Vegetational and climatic history of the Pacific Northwest during the last 20,000 years: implications for understanding present-day biodiversity. Northwest Environmental Journal, 8, 5–28.

Whitlock, C. (1993). Postglacial vegetation and climate of Grand Teton and southern Yellowstone National Parks. Ecological Monographs, 63(2), 173–198.

Williams, J. W., Shuman, B. N., Webb, T., Bartlein, P. J., & Leduc, P. L. (2004). Late-Quaternary vegetation dynamics in North America: scaling from taxa to biomes. Ecological Monographs, 74(2), 309–334.

Willing, E.-M., Dreyer, C., & van Oosterhout, C. (2012). Estimates of genetic differentiation measured by F_{ST} do not necessarily require large sample sizes when using many SNP markers. PLoS One, 7, e42649.

Wright, S. (1943). Isolation by distance. Genetics, 28, 114–138.

Yang, R. C. (1998). Estimating hierarchical *F*-statistics. Evolution, 52, 950–956.

Young, M. K., McKelvey, K. S., Jennings, T., Carter, K., Cronn, R., Keeley, E., Loxterman, J., Pilgrim, K., & Schwartz, M. K. (2017). The phylogeography of westslope cutthroat trout. bioRxiv, 213363.

Data Accessibility

Raw sequence data are deposited in the NCBI Sequence Read Archive database (BioProject XXXXXX). The DNA extraction protocol, 183-taxon genotype file with SNP calls in 012 format, species occurrence records, and R scripts used during the ENM analysis are available in our Mendeley Data accession (<http://dx.doi.org/10.17632/jhkhvdgyfy.1>).

Supporting Information

Appendix S1 Supplementary methods and results.

Data S1 Sample list, collection site details, and summary of individual assignments to genetic clusters in ADMIXTURE and DAPC analyses.

Data S2 ENM modeling results summary, including model selection results and diagnostic statistics (e.g. AUC) from ENMeval (Muscarella *et al.* 2014) and MaxEnt model metrics from ENMwizard (Heming *et al.* 2018).

Table S1 Per-locus genetic summary statistics for *P. tremuloides* and *P. trichocarpa* individuals in this study.

Table S2 Pairwise F_{ST} estimates between *P. tremuloides* genetic clusters, and their 95% confidence intervals (CIs).

Table S3 Hierarchical analysis of genetic variance among *P. tremuloides* SNPs within genetic clusters ($F_{\text{clust/total}}$), within subpopulations by cluster ($F_{\text{pop/clust}}$), and within individual trees relative to populations ($F_{\text{ind/pop}}$) and the total variance ($F_{\text{ind/total}}$). Ranges given in parentheses are 95% confidence intervals.

Figure S1 Plot of ADMIXTURE cross-validation error versus K, showing that $K = 3$ is the best fit for the full *P. tremuloides* and *P. trichocarpa* dataset of 34,796 SNPs (*sensu* Alexander & Lange 2011).

Figure S2 Plot of Bayesian information criterion (BIC) scores for k-means clustering solutions over a range of K, from the first step of DAPC, with $K = 3$ being the best solution.

Figure S3 Results of DAPC cross-validation in R establishing that the appropriate number of principal components to retain ranges from 20–100 with similarly high (>90%) prediction success.

Figure S4 DAPC loading values plotted for all 34,796 SNPs, with SNP name labels beside the SNPs with the highest loadings.

Figure S5 Genetic patterns of heterozygote and singleton alleles within and among *P. tremuloides* genetic clusters, calculated while excluding putatively admixed edge populations ($Q_{\max} < 0.75$). Results are analogous to corresponding panels of Fig. 3 (see Fig. 3 caption for details).

Figure S6 Heatmap of interindividual Nei's D estimates, reordered by row and column means, and flanked by dendrograms of the values. Color key and histogram at top left show the distribution of mean D values.

Figure S7 Heatmap of unordered interpopulation F_{ST} estimates flanked by clustering dendrograms from the distances. Color key and histogram at top left show the distribution of mean F_{ST} values.

Figure S8 Results of isolation by distance tests based on generalized linear modeling analyses of linearized F_{ST} versus log[geographic distance (km)] of *P. tremuloides* (top left) and its genetic clusters 1 (top right), 2 (bottom left), and 3 (bottom right).

Figure S9 Unrooted maximum-likelihood tree topology from the ingroup-only TreeMix analysis allowing a single migration event (A), and residual plot of the graph (B). Scale bars and legends same as in Fig. 2.

Figure S10 Results of TreeMix analyses on the full dataset conducted over varying levels of k block sizes (10 to 5000 bp) accounting for linkage disequilibrium. Scale bars and legends same as in Figs. 2 and S9.

Figure S11 Projection of the final present-day ecological niche model of *P. tremuloides* onto three late Pleistocene climatic scenarios. The ENM was built with MaxEnt and bioclimatic variables obtained from WorldClim 1, and the three Pleistocene time-slices (B–D) correspond to scenarios described in the Fig. 4 caption and Table 1. Model projections show continuous suitability values obtained using the cloglog format of MaxEnt after the application of a 10^{th}-percentile threshold. Extent of LGM ice sheets is indicated in white.

Tables and Figures

Table 1 List of climatic scenarios onto which *P. tremuloides* ecological niche models were projected. Raster files were obtained from WorldClim (Hijmans *et al.* 2005). Time period is given either as date in the Gregorian calendar system, or as thousands of years ago (ka) in the case of paleoclimatic environmental reconstructions

Climatic scenario	**Time period**	**GCM**[†]	**Resolution**[‡]	**References**
Present	1960–1990	–	2.5°	Hijmans *et al.* (2005)
Mid-Holocene (MH)	~6 ka	CCSM4	2.5°	Gent *et al.* (2011)
		IPSL-CM5A-LR		Kageyama *et al.* (2013a,b)
		MIROC-ESM		K-1 model developers (2004)
		MPI-ESM-P		Stevens *et al.* (2013)
Last Glacial Maximum (LGM)	~22 ka	CCSM4	2.5°	Gent *et al.* (2011)
		MIROC-ESM		K-1 model developers (2004)
		MPI-ESM-P		Stevens *et al.* (2013)
Last Interglacial (LIG)	~120–140 ka	NCAR-CCSM	0.5°	Otto-Bliesner *et al.* (2006)

[†]General circulation model names.

[‡]Resolutions of corresponding raster files in decimal degrees.

Table 2 Results of Mantel tests for isolation by distance investigating relationships between F_{ST} and geographical distances within *P. tremuloides*

Group	**Mantel test**	r	r^2	***p*-value**
P. tremuloides	linearized F_{ST} × log[straight-line dist. (km)]	−0.252	0.063	0.99
cluster 1	linearized F_{ST} × log[straight-line dist. (km)]	0.228	0.052	0.13
cluster 2	linearized F_{ST} × log[straight-line dist. (km)]	0.103	0.011	0.27
cluster 3	linearized F_{ST} × log[straight-line dist. (km)]	0.071	0.005	0.33

Results are shown for simple Mantel (1967) tests performed for the species as a whole, and for each of the ADMIXTURE-inferred genetic clusters within *P. tremuloides* presented in Fig. 1. Mantel's r is the standardized test statistic and is equivalent to Pearson's r, and r^2 is the coefficient of determination.

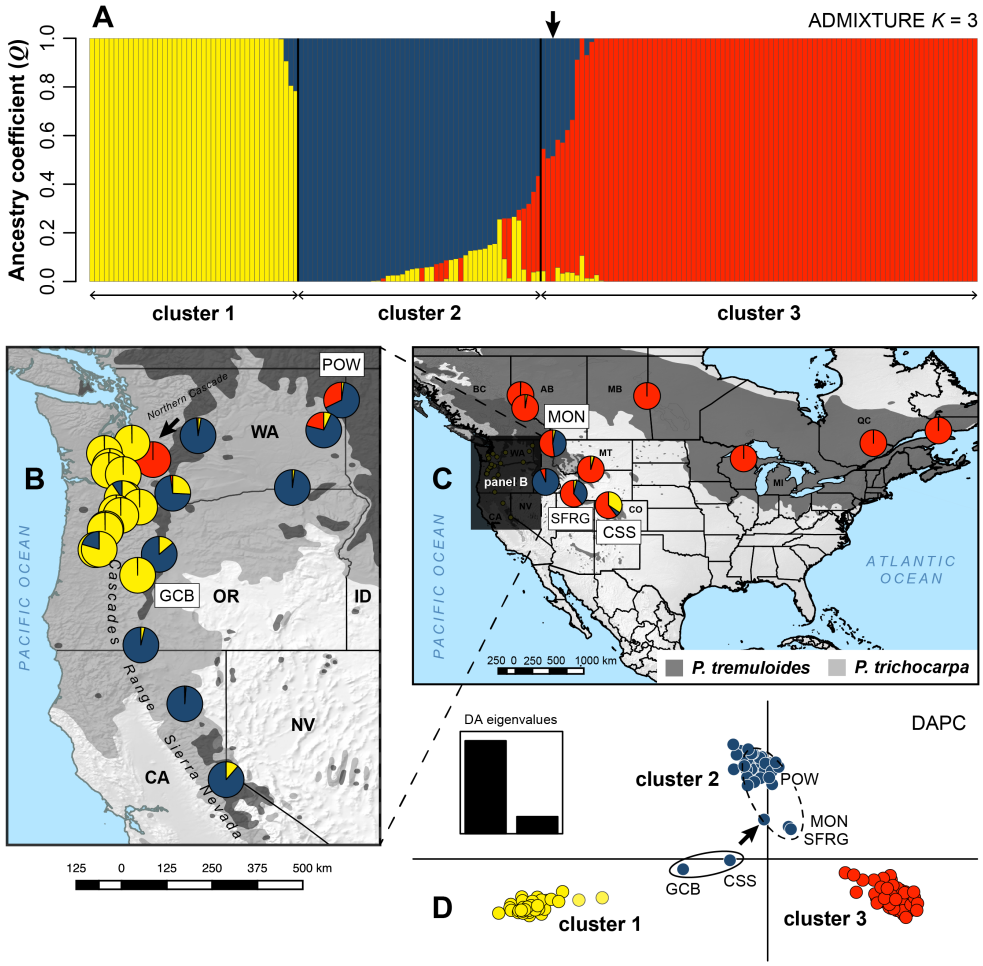

Figure 1 Map of sampling sites and patterns of population genetic structure of *Populus tremuloides* and outgroup (*P. trichocarpa*) individuals inferred from 34,796 SNP loci. Results are shown for ADMIXTURE (Alexander *et al.* 2009) assignment of individuals to each of $K = 3$ clusters (A) plotted onto topographic maps of the study area (B, C) with the present species ranges from Little (1971) shown in varying shades of gray. Pie charts show the per-site average ancestry assignment to each genetic cluster ($Q \geq 0.5$) per site and colors correspond to the ADMIXTURE barplot. Discriminant analysis of principal components (DAPC; Jombart *et al.* 2010) in adegenet (Jombart & Ahmed 2011) yielded a classification that was 95% similar to ADMIXTURE, with results plotted along the first and second discriminant functions and colored by cluster (D). Intermediate, encircled individuals in panel D were assigned to cluster 1 (solid ellipse) or cluster 3 (dotted ellipse) in ADMIXTURE. Positions of the outgroup sample are indicated by bold arrows throughout.

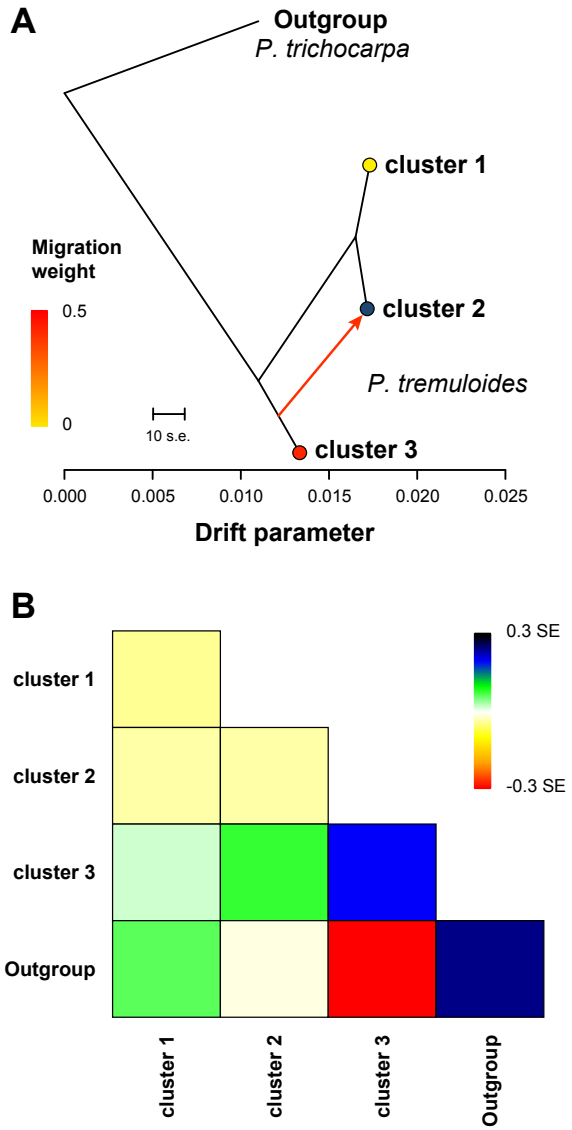

Figure 2 Phylogenomic inference of relationships among *P. tremuloides* genetic clusters, and admixture from cluster 3 into cluster 2. The final maximum likelihood tree graph inferred by phylogenomic analysis in TreeMix v1.13 (Pickrell & Pritchard 2012) allowing a single migration event (A) is presented with the migration event arrow colored by migration weight and clusters indicated by colors corresponding to Fig. 1. Scale bar: 10 times the mean standard error in the sample covariance matrix. To show putative patterns of admixture not apparent from the tree and migration edges, the residual fit of the graph is plotted and colored by the standard error color palette (B).

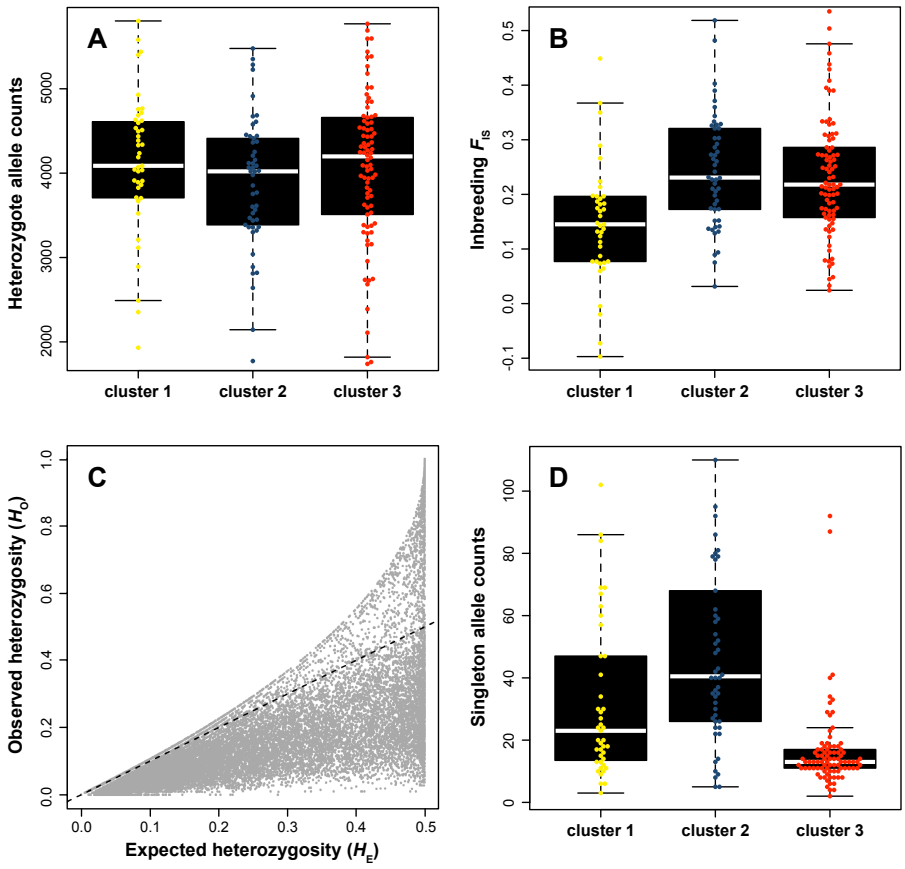

Figure 3 Genetic patterns of heterozygote and singleton alleles within and among *P. tremuloides* genetic clusters. Panels present ranges of observed numbers of heterozygote genotypes (A); ranges of inbreeding F_{IS}, a measure of heterozygote deviation from Hardy–Weinberg expectations (B); observed heterozygosity (H_{O}) plotted against expected heterozygosity (H_{E}), with deviations from 1:1 mainly below the dotted identity line (C); and ranges of observed numbers of singleton genotypes.

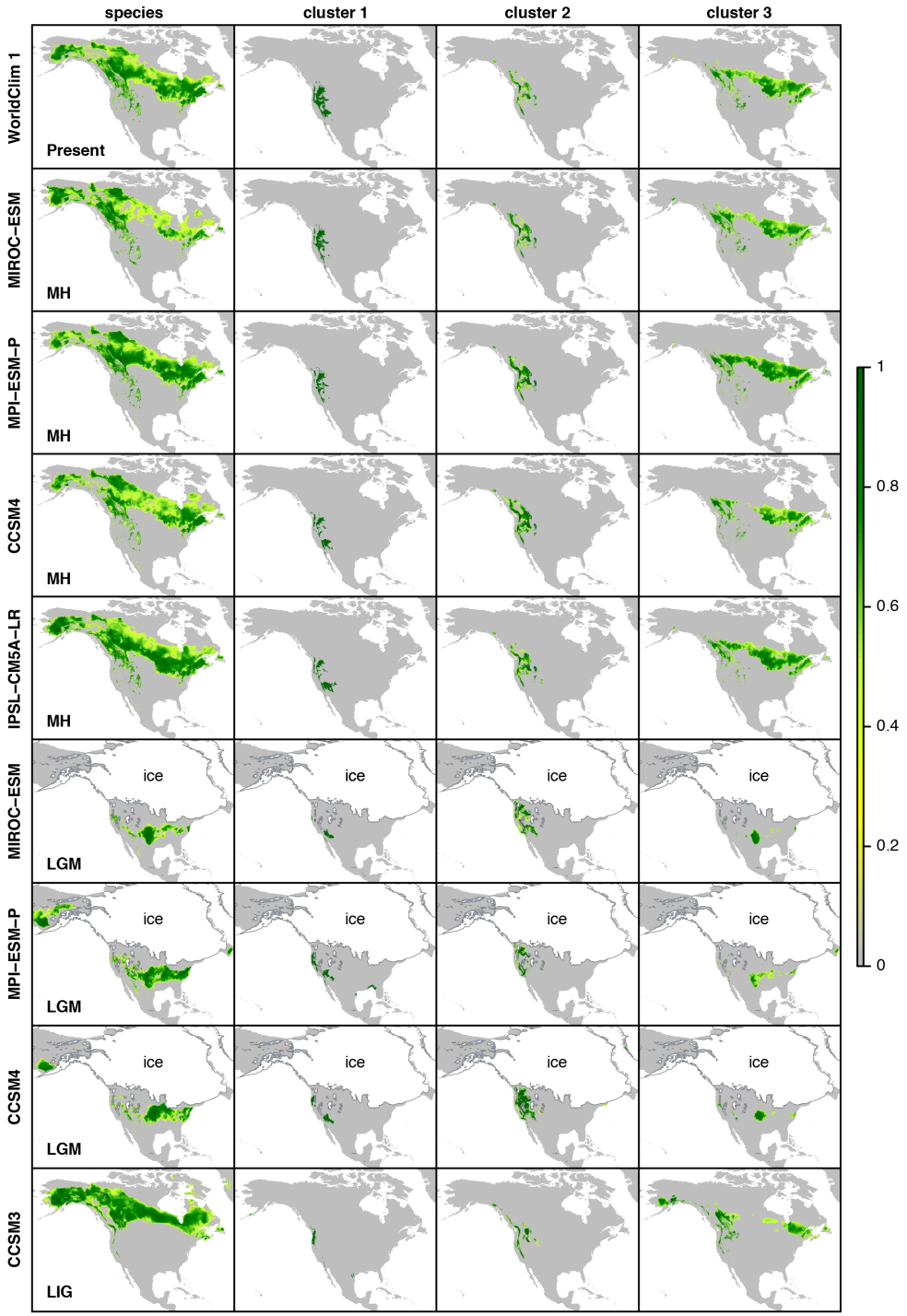

Figure 4 Predicted geographical distributions of *P. tremuloides* and its intraspecific genetic clusters from the late Pleistocene to present. MaxEnt models predicting present-day ranges of *P. tremuloides* and clusters 1–3 (top row) based on WorldClim 1 (Hijmans *et al.* 2005) were projected onto data layers for three late Pleistocene time-slices described in Table 1: Mid-Holocene (MH), Last Glacial Maximum (LGM), and Last Interglacial (LIG). Predictions are shown as color gradients from low (gray–dark yellow) to high (dark green) habitat suitability based on logistic output of the models (probability from 0 to 1), and the extent of land during each time period is shown in gray. The extent of glacial ice during the LGM is indicated in white.

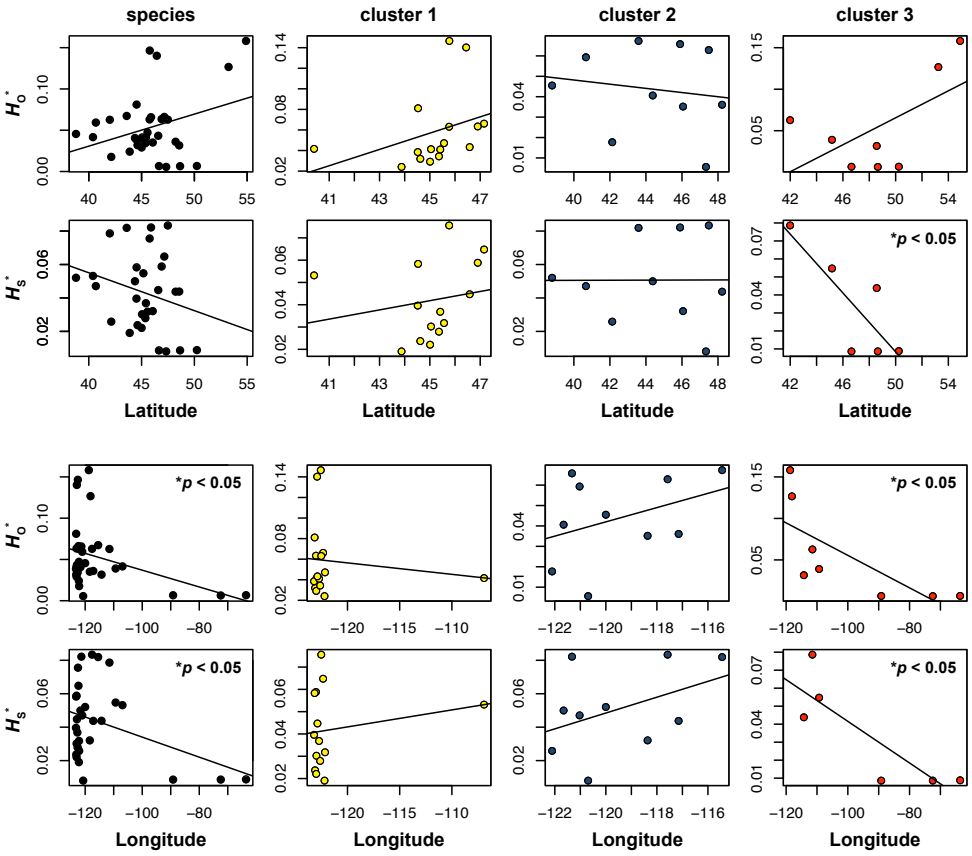

Figure 5 Latitudinal and longitudinal clines in SNP genetic diversity within *P. tremuloides* subpopulations. Linear relationships of standardized observed heterozygosity ($H_O{}^*$) and gene diversity ($H_S{}^*$) with latitude (top two rows) and longitude (bottom two rows) are presented for *P. tremuloides* as a whole, and for each ADMIXTURE-inferred genetic cluster. Each dot represents a population and is colored to match the colors of genetic clusters defined in Fig. 1, and regression lines are drawn from fitted values of generalized linear models. For significant relationships, p-values are given in the upper right of the plot.